

SUPPLEMENTARY INFORMATION



Cite this: *React. Chem. Eng.*, 2017, 2, 679

## Effect of mixing bio-oil aqueous phase model compounds on hydrogen production in non-catalytic supercritical reforming†

F. J. Gutiérrez Ortiz, \* F. J. Campanario  and P. Ollero 

**Abstract:** Bio-oil derived from biomass fast pyrolysis can be processed into fuel or some chemical products, but it has a waste aqueous phase that, however, may be valorized. Supercritical reforming of this stream, simulated using mixtures of model compounds (acetic acid, acetol, 1-butanol and glucose), was experimentally studied in a tubular reactor without using a catalyst. The effect of mixing the model compounds at different operating parameters (temperature, feed composition, and residence time) on the process performance was investigated, thus addressing an important chemical aspect of biomass-based renewable energy. The experimental dry gas composition consisted of H<sub>2</sub>, CO<sub>2</sub>, CO and CH<sub>4</sub>, although the gas yields were far from equilibrium. Hydrogen yields were normally less than 2.0 moles of H<sub>2</sub> per mole of organic feed, which are lower than those obtained for pure compounds with the same concentration. Based on the analyzed liquid samples, a series of probable reaction pathways were proposed to explain the experimental results by considering the interactions among the compounds and their formed intermediates. Thus, under tested supercritical conditions, the residence time was insufficient to reform the formed methane into hydrogen, thus leading to lower hydrogen production.

Received 23rd June 2017,  
Accepted 1st August 2017

DOI: 10.1039/c7re00090a

rsc.li/reaction-engineering

### S.1. Details on the experimental section

The analysis of liquid samples was performed using four analyzers, due to the difficulty of determining simultaneously all the tested compounds. First, it was obtained the total organic carbon (TOC) by an analyzer Shimadzu TOC-VCSH with an auto sampler ASI-V. Then, acetic acid and acetol were determined by a mass spectrometer with quadrupole analyzer Agilent (5977A low resolution) and using a gas chromatograph/mass spectrometer (Agilent 7890B) for polar capillary columns (Sapiens-5MS (30 m - 0.25 mm - 0.25 μm), Teknokroma). The analysis was performed using heating ramps during 24 min from 60 to 300 °C. The equipment used to measure the glucose is the same but using a non-polar column (19091S-433U HP-5MS UI (30 m - 0.25 mm - 0.25 μm), Agilent). Glucose was firstly derivatized with MBTFA (N-Methyl-bis trifluoroacetamide) to achieve a volatile form for glucose to be analyzed by gaseous chromatography, and then a spectral deconvolution program was applied. The analysis was performed using heating ramps during 37.5 min from 80 to 280 °C. Mass range (m/z) is between 30 and 475. In the previous analyzers and methods, 1-butanol was not detected.

This way, some of the liquid samples were analyzed by a gas chromatograph equipped with a mass spectrometry detector Ultra Shimadzu QP 2010. The analysis was performed using heating ramps during 28.5 min from 45 to 225 °C. Mass range (m/z) is between 10 and 150. Peak identification through retention time of each compound was obtained and the areas under identified peaks were computed and normalized with respect to the total area, as well as the mass-to-charge ratio for the characteristic ions. For each scan and at all the peaks detected, the following is determined: retention time, total area and % area (considering all the areas), height, width and FWHM (full width at high maximum). To identify the compounds, the library ‘Qualitative Analysis’ was used. Quantification was completed by the software named ‘MS Quantitative Analysis’. Areas under peaks are referenced to calibration. The calibration lines for each model compound were previously prepared in-house. The concentration of model compounds was determined by the area of the matching peak computed in each sample in relation to the area corresponding to the calibration line. The concentration of the identified compounds, such as, e.g., furfural or 5-HMF, was obtained by the normalized areas of the peaks of these intermediate compounds and that of the model compounds. Model compound with higher measured concentration was used as reference.

Depto. de Ingeniería Química y Ambiental, E.T.S. de Ingeniería, Universidad de Sevilla, Camino de los Descubrimientos, s/n, 41092 Sevilla, Spain.  
E-mail: frajagutor@us.es; Tel: +34 95 448 72 68/60

Structural information on an atomic scale of both crystalline and non-crystalline (amorphous) materials was acquired using XRD (Bruker D8 Advance A25 equipment). XRD analyses make it possible to determine the crystalline phase by integrating the area under all the peaks and over the background line, as well as the area under this line that corresponds to the amorphous phase, with the aid of the software DIFFRAC.EVA and the database named 'Base PDF4+ 2011' from International Centre for Diffraction Data. Likewise, carbon residues were also analyzed by electronic microscopy using SEM (PHILIPS XL-30 SEM microscope).

## S.2. Detailed reaction pathways

In order to address the discussion of the experimental results, it is convenient to establish the main reactions that may take place. This way, based on the results of previous studies and compounds detected in the liquid samples, as well as the experimental results of this study, a detailed series of probable reaction pathways is proposed (**Fig. S1**) to give insight on the interactions among the model compounds fed as a mixture.

If glucose is fed, it can follow an isomerization reaction (1) to produce fructose, and either may be dehydrated (2) to levoglucosan, as a first intermediate, that would be further converted into 5-HMF by acid catalyzed dehydration (3 or 3'), ring closure and aromatization.<sup>1</sup> Furthermore, 5-HMF may be degraded into furfural<sup>2</sup> and formaldehyde (4), which is not stable in SCW and decomposes to CO and H<sub>2</sub>. 5-HMF and furfurals are believed to trigger the polymerization reaction responsible for the formation of high molecular-weight compounds such as tar and char.<sup>3,4</sup> Furfural may form phenol via an electrocyclic reaction pathway (5).<sup>1</sup> In this way, the early formation of phenol, probably near the reactor inlet, leads to a worse performance of the SCWR due to its low reactivity, as previously pointed.<sup>5</sup> Accordingly, phenol seems to collect and stabilize free radicals thus reducing its number in the medium and, hence, the conversion of intermediates into gas. Both phenol and furfural can act as precursors of aromatic compounds (6) or polymerize (7), thus leading to the formation of unwanted tar and carbon residue, as detected in some tests of ternary and quaternary mixtures of organic constituents carried out at 700 °C and more concentrated feeding mixtures.

Nevertheless, furfural may also form a mixture of acetic acid and acrylic acid (8).<sup>6</sup> This latter would be converted into acetaldehyde by decarbonylation (9), and the acetic acid would lead to acetone (10) by ketonization or form CO<sub>2</sub> and CH<sub>4</sub> by decarboxylation at high temperature. Besides, acetic acid may be dehydrated and converted into ethanol (11) by taking four H-atoms (free radical reaction). Acrylic acid may also lead to propionic acid, as explained below.

Likewise, formic acid and levulinic acid can be obtained from 5-HMF (12), by ionic acid-catalyzed hydrolysis. Formic acid, as a small acid, decomposes preferentially into H<sub>2</sub> and

CO<sub>2</sub> (decarboxylation). Levulinic acid may be decomposed into glyoxal and acetone (13), thus increasing the amount of formed acetone from the acetic acid if this is fed, thus resulting in an interaction. Glyoxal, as a small aldehyde, is converted to CO and H<sub>2</sub> by decarbonylation.

By another pathway, glucose or fructose can produce glyceraldehyde and its less frequent isomer dihydroxyacetone (14) or, alternatively, glycolaldehyde and erythrose (15). Both pathways take place by retro-aldol condensation. Erythrose could be further transformed into glycolaldehyde by the same reaction mechanism (16) or into small aldehydes by dehydration, keto-enol tautomerization and retro-aldol condensation (17).<sup>7</sup> Normally, glycolaldehyde will decompose to H<sub>2</sub> by decarbonylation at high temperature, but it may be also converted into erythrose by aldol-condensation (18). Glyceraldehyde is decomposed to glycolaldehyde and formaldehyde (19). This latter produces H<sub>2</sub> by decarbonylation, as aforementioned, or may be transformed into formic acid and methanol through a Cannizzaro-type disproportionation reaction (20). Alternatively, glyceraldehyde may be converted into acetaldehyde and formic acid (21). These generate H<sub>2</sub>, CO, and CH<sub>4</sub>.<sup>8</sup> Methanol is reformed by SCW to CO<sub>2</sub> and H<sub>2</sub>. Alternatively, acetaldehyde may be converted into acetic acid and ethanol with SCW and by self-disproportionation (Cannizzaro reaction) (22).

Likewise, glyceraldehyde can react via pyruvaldehyde (23) to lactic acid (24), or less likely to hydroxyacetone (25) that may be also transformed into acetaldehyde and formaldehyde (26). On the other hand, lactic acid may be dehydrated to acrylic acid (27), firstly, and then to propionic acid, by free-radical reaction and adding two H-atoms (28), which produces CH<sub>4</sub> by decarboxylation.

As another pathway related to glucose, the dehydration of glyceraldehyde and dihydroxyacetone, followed by radical chain propagation, may form dienes (29). Diels-Alder cycloaddition (30) between these dienes and ethylene (coming from the decomposition of any of the other three organic compounds fed, as explained below) could give rise to cyclic structures capable of aromatization by losing hydrogen (31), as previously pointed out.<sup>9</sup> In some samples, these structures were detected.

4-hydroxy-4-methyl-2-pentanone was also identified and may be formed by dehydration of fructose plus addition of 4 H-atoms (32). Then, this intermediate would be decomposed into acetone (33). Similarly, if 5 H-atoms are added to the dehydrated fructose, 1-hexanal may be generated (34), which can be hydrogenated to 1-hexanol (35) or decomposed into acetaldehyde plus ethylene (36). Both 1-hexanal and 1-hexanol were sometimes detected.

On the other hand, when feeding acetic acid, this can be directly decomposed into methane and carbon dioxide (equimolar formation) at high temperature or it can suffer ketonization to produce acetone (10) and carbon dioxide, as above mentioned. Acetone is further decomposed into ethylene (37), carbon monoxide and hydrogen. Then, ethylene is cracked to hydrogen and carbon, which either forms methane by carbon

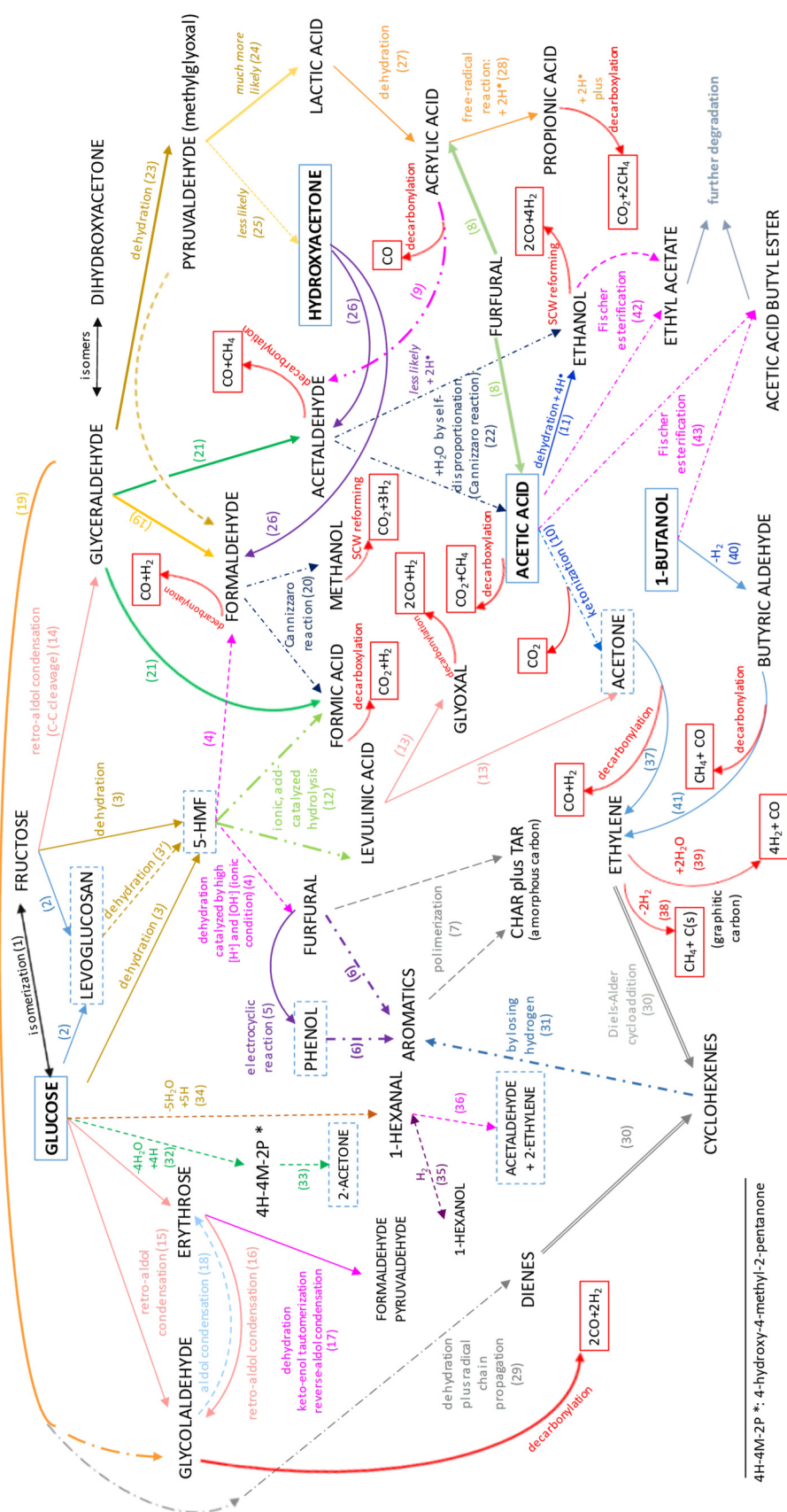


Fig. S1. Scheme of the potential reaction pathways

hydrogenation (38) or increases the hydrogen yield by carbon gasification (39). Alternatively, ethylene can react with some dienes produced as intermediates of glucose leading to cyclohexenes (30), which could derive in aromatics (31). If 1-butanol is also fed, butyric aldehyde is produced (40) and it further decomposes into methane, carbon monoxide and ethylene (41), thus increasing the effect of this intermediate on the SCWR performance. Hydroxyacetone (or acetol) decomposes into acetaldehyde and formaldehyde (26), following the above pathway, where acetic acid may also be produced (22). Ethyl acetate, which was also detected, comes from the Fischer esterification reaction of ethanol and acetic acid (42). The reaction can be accelerated by acid catalysis. Equally, acetic acid 1-butyl ester is obtained by the Fischer esterification of 1-butanol and acetic acid in an acid medium (43), which can be provided by the SCW and the acid character of the liquid products fed or formed as intermediates.

The above-described reaction pathways allow the explanation of the experimental results, especially the appearance of many organic intermediates detected in the analysis, which might interfere or interact with each other thus worsening the SCWR performance. In order to better substantiate the proposed reaction pathways, a DelPlot analysis was carried out with the available data. A first-rank Delplot analysis<sup>10</sup> allows the discrimination between primary and non-primary reaction products, thus supporting the potential set of reaction pathways. This plot represents normalized selectivity, defined as molar yield of a product divided by conversion of each reactant in mixture, versus conversion of each reactant in mixture. In this study, conversion values were almost complete in most of tests, and selectivity values were close to zero for any product considered as intermediate, so this analysis could not be performed for all the reaction sequences, and no Figure is shown. The extrapolation of the data on this plot to zero conversion from almost the unity is not clearly conclusive because almost all the values of ordinate axis are very low and grouped around the unity. Despite this limitation of the Delplot analysis in this study, for some compounds, such as hexanol, ethanol, and methanol, the y-intercept seems to be around zero, which indicates that the quantified reaction products are secondary, tertiary, etc. Thus, although the Delplot analysis was inconclusive, some pieces of information obtained support the potential reaction network.

### S.3. Effect of the operating parameters

**Fig. S2-S4** depict the effect of the residence time and the concentration of some binary and ternary mixtures of organic constituents, without glucose, on the yield of hydrogen and other gases, at 800 °C. The solid and dashed lines represent equilibrium values, where a complete feedstock conversion is achieved.

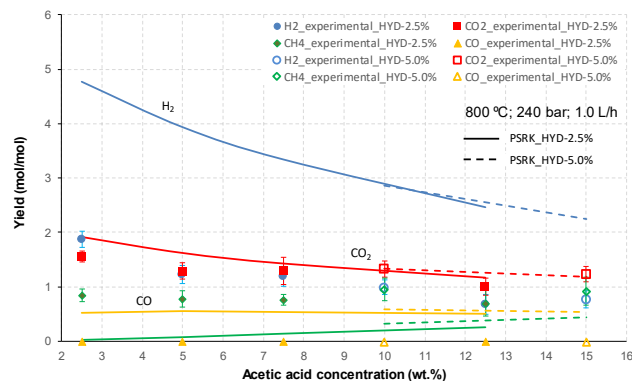


**Fig. S2.** Effect of the acetic acid concentration on the gas yields for two different hydroxyacetone concentrations (2.5 and 5.0 wt.%), at 800 °C, 240 bar and 1.0 L/h [H<sub>2</sub>: blue; CO<sub>2</sub>: red; CH<sub>4</sub>: green; CO: orange].

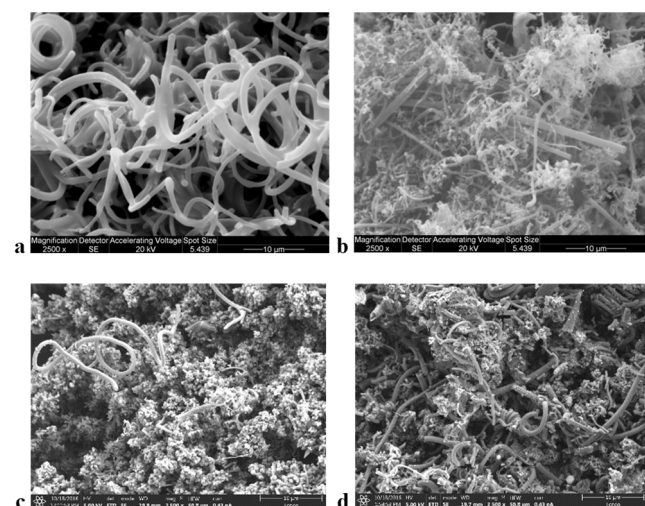
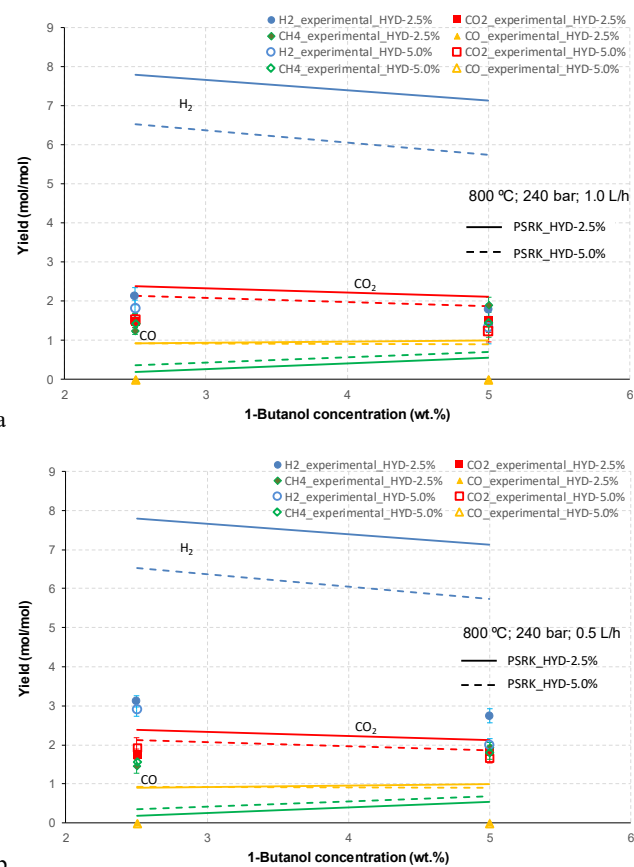
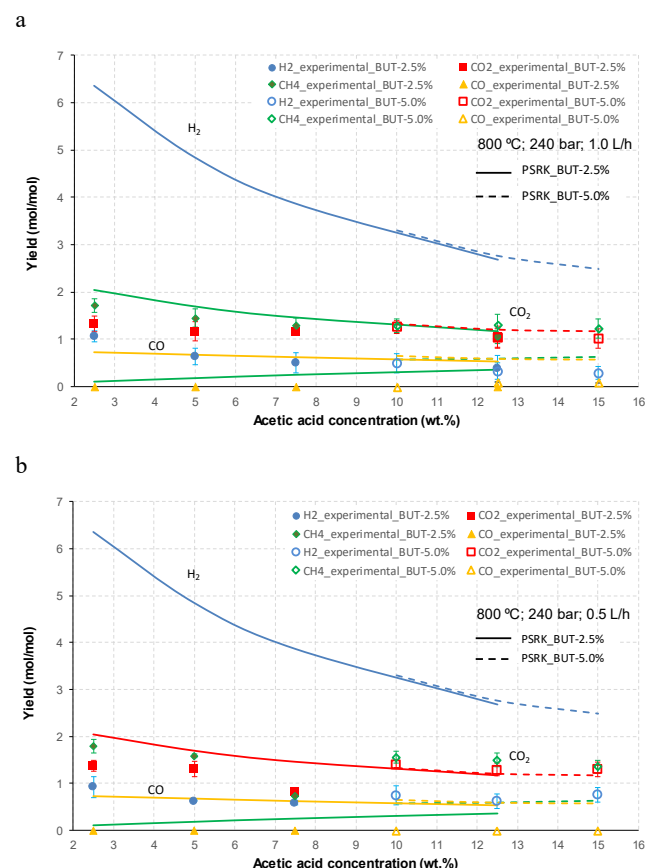
### S.4. Solid carbon characterization

Regarding the solid phase, amorphous carbon was mainly detected in those tests where char was likely formed by glucose decomposition to char (amorphous carbon) via furfural, phenol and aromatics (polymerization reaction 7, in **Fig. S1**). Thus, 5-HMF and aromatic liquid products polymerize to form water-insoluble char particles, mostly via the reactions of ring substitution and the substituent functional groups.<sup>4</sup> Similarly, the hydrogenation of phenol to form benzene and further to cyclohexane may lead to the formation of large amount of intermediate product by ring-openings, and in the presence of carboxylic acid (such as acetic acid), a favourable condition for esterification and polymerization reactions can be provided, as previously suggested.<sup>11</sup> Thus, the most probable mechanism for amorphous char formation is by polymerization reactions derived from phenol and furfural formed as of 5-HMF. These reactions are boosted in the presence of acetic acid.

On the other hand, the amount of formed graphitic carbon varied depending on the fed organic compounds and the operating conditions, so solid carbon may also come from the cracking of ethylene formed during the progressive transformation of the organic compounds (reactions 37 and/or 41 in **Fig. S1**), especially from acetic acid and 1-butanol. The formed solid carbon may undergo gasification to CO and H<sub>2</sub> (reaction 39 in **Fig. S1**) or hydrogenation to produce CH<sub>4</sub> (reaction 38 in **Fig. S1**). This may explain that the solid carbon formation was greater at 700 °C than at 800 °C, because solid carbon gasification to CO and H<sub>2</sub> is favored at high temperature.

**Fig. S5** presents SEM micrographs of carbonaceous residue for four mixtures. In the SEM images, the structures of carbon nanotubes are clearly observed in samples of the binary mixture of acetic acid and 1-butanol (a) and the ternary mixture of acetic acid, 1-butanol and hydroxyacetone (b), as well as in the ternary mixture of acetic acid, 1-butanol and glucose (c) and the quaternary mixture (d). In case (a), the carbon nanotubes are quite homogeneous while, in case (b), more heterogeneous carbon filaments are observed. On the other hand, for the two

mixtures with glucose, apart from carbon nanotubes of different shape and size, granules and other shapes of carbon are also seen, even more frequently. By XRD analyses, the percentage of each detected and identified crystalline phase is performed by measuring the Y-scale value and correcting the intensity of the peak with that of corundum. This also allows the calculation of the ratio between two crystalline phases, such as the graphite-to-carbon ratio. **Fig. S6** shows the XRD pattern for the sample of ternary mixture (a), where the crystalline phase is quite higher than the amorphous phase (65.6/34.4) but the graphite-to-carbon ratio in the crystalline phase was only 0.08, which is quite lower than 1.0. Likewise, the sample of quaternary mixture (b) showed a crystalline phase of 56.9% and an amorphous phase of 43.1%, with a graphite-to-carbon ratio in the crystalline phase of 1.10. Thus, and although Raman spectroscopy should be employed to accurately investigate the nature of carbon, it seems that the quaternary mixture is relatively better graphitized although the crystalline phase is lower than that of the ternary mixture. In this way, when acetol is present in the mixture, less solid carbon is formed and this is well graphitized, while 1-butanol and glucose tend to form larger amounts of solid carbon, which is less graphitized. This probably occurs because both glucose and 1-butanol can suffer further degradation to amorphous carbon, while acetol reforms quite well or could lead to carbon from ethylene hydrogenation, as included in the reaction pathways (reaction 38).



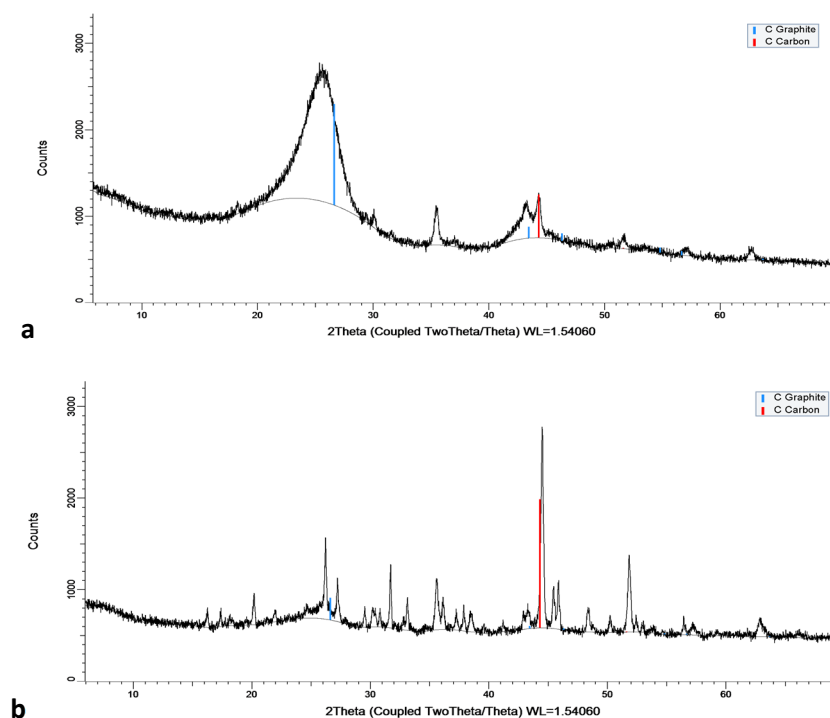


**Fig. S6.** XRD of solid carbon for mixtures of: (a) acetic acid, 1-butanol and glucose; and (b) quaternary (15 wt.% acetic acid and 2.5 wt.% for the rest of feed compounds, at 800 °C, 240 bar and 1.0 L/h)

## References

- 1 A. Sinag, A. Kruse, V. Schwarzkopf. Key compounds of the hydrolysis of glucose in supercritical water in the presence of  $K_2CO_3$ , *Ind. Eng. Chem. Res.* 2003, 42, 3516-3521.
- 2 A. Kruse, A. Gawlik. Biomass conversion in water at 330–410 °C and 30–50 MPa. Identification of key compounds for indicating different chemical reaction pathways. *Ind. Eng. Chem. Res.* 2003, 42, 267–279.
- 3 J.T. Henrikson, Z. Chen, P.E. Savage. Inhibition and acceleration of phenol oxidation by supercritical water. *Ind. Eng. Chem. Res.* 2003, 42, 6303–6309.
- 4 A. Chuntanapum, T.L.-K. Yong, S. Miyake, Y. Matsumura. Behavior of 5-HMF in Subcritical and Supercritical Water. *Ind. Eng. Chem. Res.* 2008, 47, 2956-2962.
- 5 G.J. DiLeo, M.E. Neff, S. Kim, P.E. Savage. Supercritical water gasification of phenol and glycine as models for plant and protein biomass. *Energ. Fuel* 2008, 22, 871–877.
- 6 Q. Jing, X. Lü. Kinetics of Non-Catalyzed Decomposition of D-Xylose in High Temperature Liquid Water. *Chin. J. Chem. Eng.* 2007, 15, 666-669.
- 7 H. Kishida, F. Jin, X. Yan, T. Moriyac, H. Enomoto. Formation of lactic acid from glycolaldehyde by alkaline hydrothermal reaction. *Carbohydr. Res.* 2006, 341, 2619–2623.
- 8 F.J. Gutiérrez Ortiz, A. Serrera, S. Galera, P. Ollero. Experimental study of the supercritical water reforming of glycerol without the addition of a catalyst. *Energy* 2013, 56, 193-206.
- 9 M.B. Korzenski, J.W. Bolis. Diels-Alder Reactions Using Supercritical Water as an Aqueous Solvent Medium. *Tetrahedron Lett.* 1997, 38, 5611-5614.
- 10 N. Bhore, M. Klein. The Delplot technique: A new method for reaction pathways analysis. *Ind. Eng. Chem. Res.* 1990, 29, 313-316.
- 11 Y. Guo, S.Z. Wang, Y.Z. Wang, J. Zhang, D.H. Xu, Y.M. Gong. Gasification of two and three-components mixture in supercritical water, influence of NaOH and initial reactants of acetic acid and phenol. *Int. J. Hydrogen Energ.* 2012, 37, 2278–2286.